NJC

Check for updates

Electron transfer between neptunium and sodium chlorite in acidic chloride media†

Brian T. Arko, [ab] David Dan,[a] Sara L. Adelman, *[a] David B. Kimball, *[a] Stosh A. Kozimor *[a] and Jenifer C. Shafer *[b]

Controlling aqueous 5f-element electron transfer chemistry is critical for processing efforts associated with actinide technologies. Often, redox agents are added during actinide processing steps to control actinide redox chemistry and manipulate the actinide oxidation states for the separation. Sodium chlorite, $NaClO_{2(aq)}$, represents one of these useful redox agents. For example, $NaClO_{2(aq)}$ finds widespread application in the processing of plutonium and americium. Surprisingly, however, redox reactivity between $NaClO_{2(aq)}$ and other actinides, like neptunium, has been largely ignored. That knowledge gap is addressed herein. We characterized some redox reactivity between $NaClO_{2(aq)}$ and $Np^{4+}_{(aq)}$ and identified experimental conditions that held neptunium in the +4 oxidation state or converted $Np^{4+}_{(aq)}$ to $NpO_2^{2+}_{(aq)}$ or $NpO_2^{1+}_{(aq)}$. This was achieved by carefully adjusting four variables: ingoing concentrations of (1) $Np^{4+}_{(aq)}$, (2) $NaClO_{2(aq)}$, (3) $Cl^{1-}_{(aq)}$, and (4) $H^{1+}_{(aq)}$. We discovered that three neptunium oxidation states (+4, +5, and +6) could be accessed using one ubiquitous redox agent, $NaClO_{2(aq)}$. These results highlight the diverse electron transfer chemistry available to neptunium in aqueous solutions, provide new insight on how neptunium reacts with $NaClO_{2(aq)}$, and are discussed within the context of their importance to plutonium and americium processing.

Introduction

Controlling electron transfer chemistry accessible to the 5f-elements in aqueous media is critical for nearly every actinide-based technological application. These applications span from isotope production, environmental restoration, nuclear fuel rod fabrication, space exploration, and harvesting actinides from weapons program waste streams.[1–19] The latter topic was the major motivating factor for this particular research effort. For instance, at Los Alamos National Laboratory (LANL), transuranic actinides – like plutonium (Pu) and americium (Am) – are recovered from aqueous waste streams.[20–23] Success associated with this waste stewardship is valuable and responsible. It reduces burden on taxpayers by lowering transuranic waste costs, decreases the amount of transuranic waste generated, and recycles valuable and rare radioisotopes (*e.g.*, ^{238}Pu, ^{239}Pu, ^{240}Pu, ^{241}Pu, ^{242}Pu, and ^{241}Am) for national security and industrial usage.

To recover plutonium and americium from aqueous waste streams, LANL implemented the experimental chloride extraction line (EXCEL) and chloride extraction and recovery (CLEAR)

aqueous processing methods.[15,24–28] In terms of plutonium recovery, waste entering the processing line contains plutonium in a variety of oxidation states. Hence, successful plutonium recovery requires a valence state adjustment that holds plutonium in the +4 oxidation state during subsequent chemical processing steps. This plutonium oxidation-state adjustment can be carried out using sodium chlorite; $NaClO_{2(aq)}$. The robustness associated with using $NaClO_{2(aq)}$ as a plutonium valence adjusting agent has been documented by the successful recovery of plutonium from diverse waste streams using EXCEL for decades.[16,29]

Accompanying changes to the national nuclear agenda, described in the Nuclear Posture Review, are new chemical challenges that face aqueous recovery and recycling of plutonium and americium.[30–32] One obstacle is associated with needs to accommodate increasingly diverse waste feedstocks. Processing these feedstocks is complicated because they contain a wide range of chemical constituents. In addition, their chemical identities and quantities change with time. One relevant example is neptunium-237: ^{237}Np, half-life ($t_{1/2}$) = 2.144(7) × 10^6 y.[33] Concerns regarding ^{237}Np contamination stem from substantial ^{237}Np ingrowth in aged plutonium/americium containing waste. Fig. 1 qualifies these concerns. It shows that the ^{237}Np contaminant is generated *via* α-decay from its ^{241}Am [$t_{1/2}$ = 432.6(6) y] parent radionuclide, which in turn is the β$^-$ decay product from ^{241}Pu [$t_{1/2}$ = 14.329(29) y].[33] It also highlights how "aged" waste will contain substantial

^{a} *Los Alamos National Laboratory, Los Alamos, NM 87545, USA.*
 E-mail: dkimball@lanl.gov, stosh@lanl.gov; Web: https://sadelman@lanl.gov
^{b} *Department of Chemistry, Colorado School of Mines, Golden, CO 90401, USA.*
 E-mail: jshafer@mines.edu
† Electronic supplementary information (ESI) available. See DOI: https://doi.org/10.1039/d3nj03730d
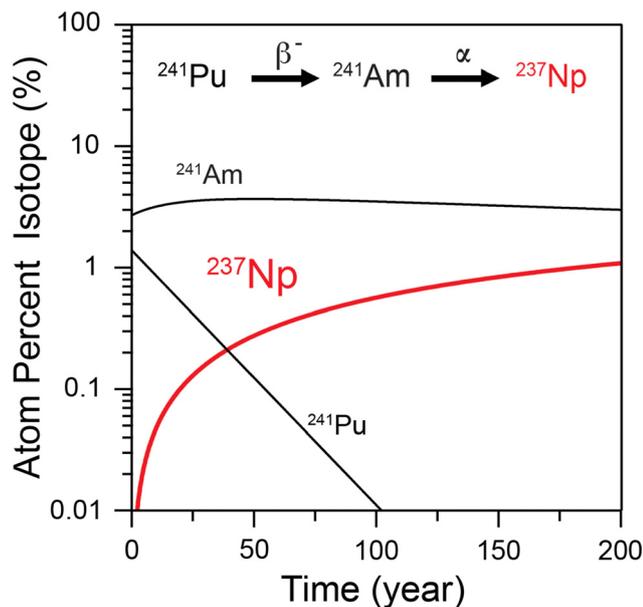
Fig. 1 Calculated isotopic decay products for selected transuranic radio-isotopes within aged plutonium calculated from aged plutonium isotopic content (WGPu-C, 16–19% ^{240}Pu as defined in the compendium of material composition data for radiation transport modeling).[39]

quantities of ^{237}Np.[34–38] Unfortunately, it is unknown how ^{237}Np$_{(aq)}$ will respond to the antecedently described plutonium valence adjustment step because redox chemistry between neptunium and NaClO$_{2(aq)}$ has not been studied in depth. Defining electron transfer chemistry between neptunium and NaClO$_{2(aq)}$ in aqueous solutions is relevant to plutonium/americium processing. That information will show how ^{237}Np contaminants move through the EXCEL and CLEAR processing lines and provide insight for maintaining robustness and effectiveness in plutonium/americium waste processing efforts.

To address the aforementioned ^{237}Np processing concerns, we set out to characterize some redox chemistry between ^{237}Np$_{(aq)}$ and the NaClO$_{2(aq)}$. We discovered that we could force neptunium into three different oxidation states (+4, +5, +6) using the NaClO$_{2(aq)}$ redox agent by manipulating four experimental variables. Those variables were ingoing concentrations of Np$^{4+}_{(aq)}$, NaClO$_{2(aq)}$, Cl$^{1-}_{(aq)}$, and H$^{1+}_{(aq)}$. Although α-particle radiation has been known to influence neptunium oxidation state chemistry, these attributes were not considered.[40] Scheme 1 and Table 1 showcase that NaClO$_{2(aq)}$ acted as a Np$^{4+}_{(aq)}$ valence holding agent under a wide range of experimental conditions. We also found experimental conditions that converted Np$^{4+}_{(aq)}$ to the NpO$_2^{1+}_{(aq)}$ mono-cation or the NpO$_2^{2+}_{(aq)}$ di-cation. Stable solutions of NpO$_2^{1+}_{(aq)}$ were obtained when the ingoing concentrations of Np$^{4+}_{(aq)}$ (0.81 mM), NaClO$_{2(aq)}$ (3.4 mM), Cl$^{1-}_{(aq)}$ (0.026 M), and H$^{1+}_{(aq)}$ (0.02 M) were all relatively low. Stable solutions of NpO$_2^{2+}_{(aq)}$ were obtained when the ingoing concentration of Np$^{4+}_{(aq)}$ was high (3.1 mM to 1.5 mM), NaClO$_{2(aq)}$ was high (160 to 32 mM), Cl$^{1-}_{(aq)}$ ranged 0.02 to 9.2 M, and H$^{1+}_{(aq)}$ was between 0.02 and 5.4 M. Overall, these results demonstrated that that reactivity between Np$^{4+}_{(aq)}$ and NaClO$_{2(aq)}$ was diverse,
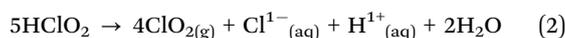
predictable, and therefor controllable. That insight advances understanding about neptunium electron transfer reactions under experimental conditions that are relevant to those described above during EXCEL and CLEAR processing of plutonium and ^{241}Am.

Before discussing reactivity between Np$^{4+}_{(aq)}$ and NaClO$_{2(aq)}$, we found it instructive to comment – at a high level – on the aqueous reactivity of NaClO$_{2(aq)}$ in Cl$^{1-}_{(aq)}$ containing solutions. The chemistry of NaClO$_{2(aq)}$ has been the subject of numerous experimental studies described previously.[41–47] The NaClO$_2$ salt has been structurally characterized.[48–50] The ClO$_2^{1-}$ anion contains chlorine in the +3 oxidation state, and (based on the standard half-cell potentials) is the strongest oxidizer in the chlorine oxyanion family.[45] As testament, many salts containing the ClO$_2^{1-}$ anion are reported to decompose explosively when exposed to heat and shock, e.g. salts of Ag^{1+}, Hg^{1+}, Tl^{1+}, Pb^{2+}, Cu^{2+}, and NH$_4^{1+}$.[51] Hence, inorganic ClO$_2^{1-}$ salts are often regarded as being unstable and highly reactive. In aqueous solutions, the conjugate acid of ClO$_2^{1-}$ (chlorous acid; HClO$_2$) is a weak acid (p$K_a \sim 1.94$),[52] one of the most reactive (least stable) oxoacids of chlorine,[53] and has only been observed in aqueous solution at low concentrations.[54] In aqueous chloride solutions, the chemistry of the ClO$_2^{1-}_{(aq)}$/HClO$_2(aq)$ pair is dominated by disproportionation reactions whose product ratios are heavily influenced by the H$^{1+}_{(aq)}$ and Cl$^{1-}_{(aq)}$ concentrations associated with the aqueous matrix.[47,55–57] For example, in aqueous matrixes and in the absence of Cl$^{1-}_{(aq)}$, the ClO$_2^{1-}_{(aq)}$ anion is reported to disproportionate and form gaseous chlorine dioxide [Cl^{IV}O$_{2(g)}$], chlorate [Cl^{V}O$_3^{1-}_{(aq)}$], and chloride [Cl$^{1-}_{(aq)}$] (eqn (1)). In contrast, when Cl$^{1-}_{(aq)}$ concentrations are high (see ref. 58 for details), the disproportionation reaction favors formation of the ClO$_{2(g)}$ and Cl$^{1-}_{(aq)}$ pair (eqn (2)) and the formation of ClO$_3^{1-}_{(aq)}$ is suppressed. According to Kieffer and Gordon, the rate of ClO$_2^{1-}_{(aq)}$ disproportionation also varies with Cl$^{1-}_{(aq)}$ content. For example the disproportionation reaction rate increases substantially when moving from low (no ingoing) Cl$^{1-}_{(aq)}$ concentration ($t_{1/2}$ = 389 $\pm$ 3 min without added Cl$^{1-}_{(aq)}$) to higher (100 mM) Cl$^{1-}_{(aq)}$ concentrations ($t_{1/2}$ = 6.85 $\pm$ 0.05 min).[56,57] These disproportionation rates are not exact, and likely represent a combination of multiple chemical events and intertwined reactions.[58]

ClO$_2^{1-}_{(aq)}$ disproportionation in low Cl$^{1-}_{(aq)}$ conditions

$$4HClO_2 \rightarrow 2ClO_{2(g)} + ClO_3^{1-}_{(aq)} + Cl^{1-}_{(aq)} + 2H^{1+}_{(aq)} + H_2O \quad (1)$$
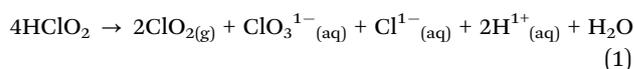
ClO$_2^{1-}_{(aq)}$ disproportionation in high Cl$^{1-}_{(aq)}$ conditions

$$5HClO_2 \rightarrow 4ClO_{2(g)} + Cl^{1-}_{(aq)} + H^{1+}_{(aq)} + 2H_2O \quad (2)$$

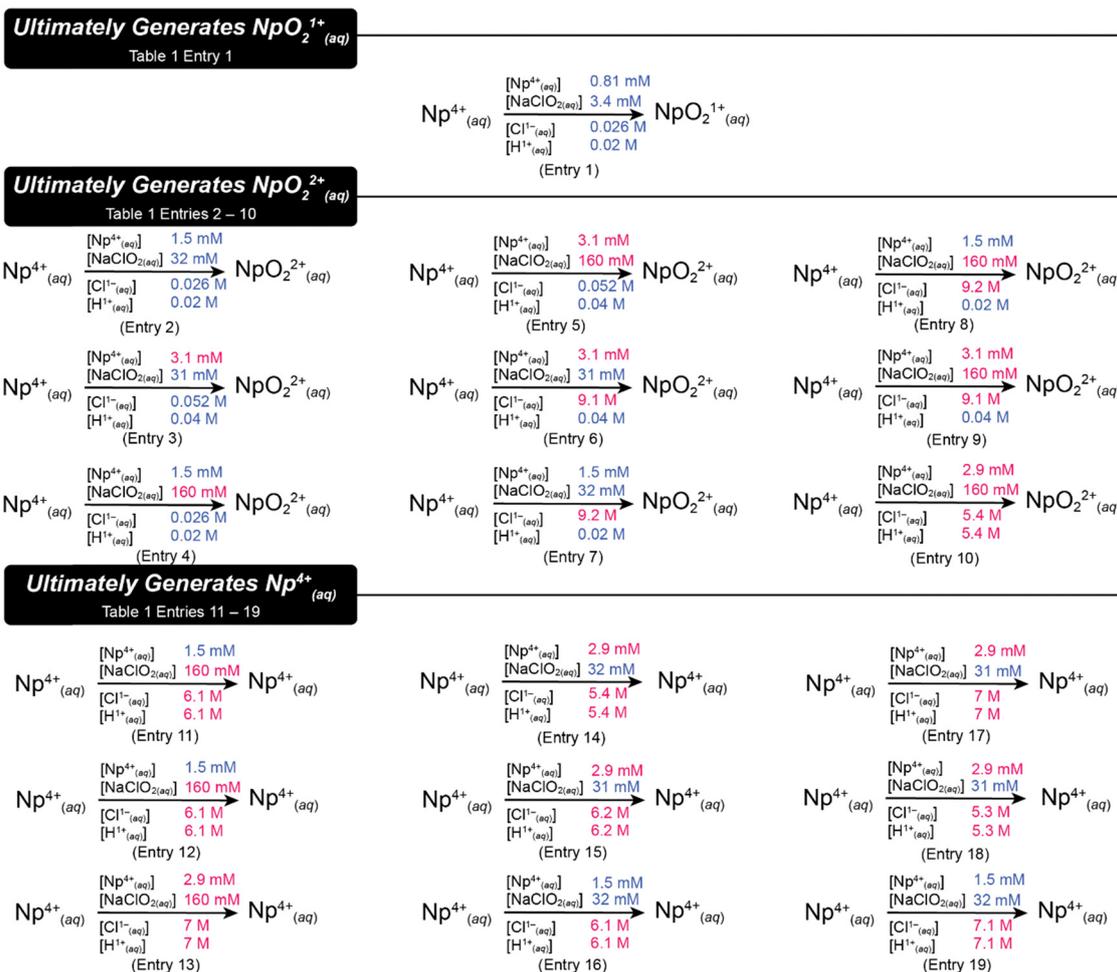## Results and discussion

Generating oxidation state pure solutions of NpO$_2^{1+}_{(aq)}$ and NpO$_2^{2+}_{(aq)}$ with NaClO$_{2(aq)}$

We discovered experimental conditions that selectively oxidized Np$^{4+}_{(aq)}$ to either NpO$_2^{1+}_{(aq)}$ or NpO$_2^{2+}_{(aq)}$ in aqueous acidic solutions of HCl$_{(aq)}$ (0.02 to 5.4 M; entries 1 to 10 in Table 1)

Scheme 1 General $Np^{4+}_{(aq)}$ reaction products under various experimental conditions. The "entry" showed in parentheses references the experimental conditions documented in Table 1. Colors associated with concentrations are depicted as relatively high or low.

without the exclusion of air. To carry out these studies, we generated an oxidation state and chemically pure aqueous stock solution of $Np^{4+}_{(aq)}$ (66 mM) using a previously described method.[59] Aliquots from this $Np^{4+}_{(aq)}$ stock solution were combined with the $NaClO_{2(aq)}$ oxidant at fixed $Cl^{1-}_{(aq)}$ concentrations. Transformations that converted $Np^{4+}_{(aq)}$ to either $NpO_2^{1+}_{(aq)}$ and/or $NpO_2^{2+}_{(aq)}$ were subsequently monitored using ultraviolet-visible (UV-vis) absorption spectroscopy. Scheme 1 and Table 1 provide a high-level summary of how the matrix compositions impacted product formation.

We found that exclusive formation of $NpO_2^{1+}_{(aq)}$ occurred when ingoing concentrations for the $^{237}Np_{(aq)}$ analyte (0.81 mM), $NaClO_{2(aq)}$ redox agent (3.4 mM), $Cl^{1-}_{(aq)}$ complexing agent (0.026 M), and $H^{1+}_{(aq)}$ (0.02 M) were all low, relative to the other experimental conditions we examined (entry 1 in Table 1). As documented in Fig. 2, addition of $NaClO_{2(aq)}$ to a solution of $Np^{4+}_{(aq)}$ caused the UV-vis absorption peaks from $Np^{4+}_{(aq)}$ at $10\,500\ cm^{-1}$ (960 nm) and $8700\ cm^{-1}$ (1150 nm) to vanish within 1 day (see Fig. 3). Concomitantly, new peaks from $NpO_2^{1+}_{(aq)}$ at $10\,200\ cm^{-1}$ (980 nm) and $9100\ cm^{-1}$ (1100 nm) emerged. Fig. 2 and 3 additionally documented that this

$NpO_2^{1+}_{(aq)}$ product was stable during a 5-day monitoring process, as no other neptunium oxidation states were detected by UV-vis spectroscopy. To obtain additional insight into the transformation of $Np^{4+}_{(aq)}$ to $NpO_2^{1+}_{(aq)}$, we characterized the rate at which absorption peaks from $Np^{4+}_{(aq)}$ decreased in intensity and peaks associated with $NpO_2^{1+}_{(aq)}$ were prevalent for 5 days (Fig. 3). The reaction rate laws were calculated, and subsequent analyses suggested that oxidation of $Np^{4+}_{(aq)}$ to $NpO_2^{1+}_{(aq)}$ proceeded by fractional order dependence on both the $Np^{4+}_{(aq)}$ and $ClO_2^{1-}_{(aq)}$ reagents, 0.300 ± 0.008 and 0.110 ± 0.002, respectively. Fractional order reactions can be indicative of chain reactions propagated by radical species present in solution and many radical reactions pathways could be responsible for the $NaClO_{2(aq)}$ initiated conversion of $Np^{4+}_{(aq)}$ to $NpO_2^{1+}_{(aq)}$.[41,60–63]

Subtle changes in the aqueous matrix identity substantially impacted the $Np^{4+}_{(aq)}$ oxidation process. As a representative example, data displayed in Fig. 4 documented how oxidizing $Np^{4+}_{(aq)}$ to $NpO_2^{1+}_{(aq)}$ was dependent on the ingoing $NaClO_{2(aq)}$ quantities. To generate these data, we sequentially added aliquots of $NaClO_{2(aq)}$ (0.072 μmol; 10 μL of a 7.2 mM stock solution) to an

Table 1 Experimental conditions associated with all reactions between $Np^{4+}_{(aq)}$ and $NaClO_{2(aq)}$ described in this paper. Ingoing concentrations of $Np^{4+}_{(aq)}$, $NaClO_{2(aq)}$, $H^{1+}_{(aq)}$, and $Cl^{1-}_{(aq)}$ are recorded. Also shown is the dominant neptunium species that forms at two different time points (after 1 *vs.* 24 h). Note, ingoing $Cl^{1-}_{(aq)}$ concentration includes three sources: from $HCl_{(aq)}$, from LiCl, and from the ingoing $Np^{4+}_{(aq)}$ stock solution. Values in the "Ingoing Cl^{1-} Total (M)" concentration column represent total ingoing Cl^{1-} concentration (top number), the contributions from $HCl_{(aq)}$ and $LiCl_{(aq)}$ (bottom numbers in parentheses), and contributions from the $Np^{4+}_{(aq)}$ stock solution

Entry	Dominant species (t = 1 h)	Dominant species (t = 24 h)	Initial $Np^{4+}_{(aq)}$ (mM)	Initial $NaClO_{2(aq)}$ (mM)	Initial $H^{1+}_{(aq)}$ (M)	Ingoing Cl^{1-} total[a] (M) (Cl^{1-} from HCl) + (Cl^{1-} from LiCl) + (Cl^{1-} from NpCl$_4$)
1	$NpO_2^{1+}_{(aq)}$	$NpO_2^{1+}_{(aq)}$	0.81	3.4	0.02	0.023 (0.02) + (0) + 0.003
2	$NpO_2^{1+}_{(aq)}$	$NpO_2^{2+}_{(aq)}$	1.5	32	0.02	0.026 (0.02) + (0) + 0.006
3	$NpO_2^{1+}_{(aq)}$	$NpO_2^{2+}_{(aq)}$	3.1	31	0.04	0.052 (0.04) + (0) + 0.012
4	$NpO_2^{1+}_{(aq)}$	$NpO_2^{2+}_{(aq)}$	1.5	160	0.02	0.026 (0.02) + (0) + 0.006
5	$NpO_2^{1+}_{(aq)}$	$NpO_2^{2+}_{(aq)}$	3.1	160	0.04	0.052 (0.04) + (0) + 0.012
6	$Np^{4+}_{(aq)}$	$NpO_2^{2+}_{(aq)}$	3.1	31	0.04	9.1 (0.04) + (9.0) + 0.012
7	$Np^{4+}_{(aq)}$	$NpO_2^{2+}_{(aq)}$	1.5	32	0.02	9.2 (0.02) + (9.2) + 0.006
8	$Np^{4+}_{(aq)}$	$NpO_2^{2+}_{(aq)}$	1.5	160	0.02	9.2 (0.02) + (9.2) + 0.006
9	$Np^{4+}_{(aq)}$	$NpO_2^{2+}_{(aq)}$	3.1	160	0.04	9.1 (0.04) + (9.0) + 0.012
10	$Np^{4+}_{(aq)}$	$NpO_2^{2+}_{(aq)}$	2.9	160	5.4	5.4 (5.4) + (0) + 0.012
11	$Np^{4+}_{(aq)}$	$Np^{4+}_{(aq)}$	1.5	160	6.1	6.1 (6.1) + (0) + 0.006
12	$Np^{4+}_{(aq)}$	$Np^{4+}_{(aq)}$	1.5	160	7.1[e]	7.1 (7.1) + (0) + 0.006
13	$Np^{4+}_{(aq)}$	$Np^{4+}_{(aq)}$	2.9	160	7	7.0 (7.0) + (0) + 0.012
14	$Np^{4+}_{(aq)}$	$Np^{4+}_{(aq)}$	2.9	32	5.4	5.4 (5.4) + (0) + 0.012
15	$Np^{4+}_{(aq)}$	$Np^{4+}_{(aq)}$	2.9	31	6.2	6.2 (6.2) + (0) + 0.012
16	$Np^{4+}_{(aq)}$	$Np^{4+}_{(aq)}$	1.5	32	6.1	6.1 (6.1) + (0) + 0.006
17	$Np^{4+}_{(aq)}$	$Np^{4+}_{(aq)}$	2.9	31	7.0	7.0 (7.0) + (0) + 0.012
18	$Np^{4+}_{(aq)}$	$Np^{4+}_{(aq)}$	2.9	31	5.3	5.4 (5.4) + (0) + 0.012
19	$Np^{4+}_{(aq)}$	$Np^{4+}_{(aq)}$	1.5	32	7.1	7.1 (7.1) + (0) + 0.006

[a] Calculations show ingoing $Cl^{1-}_{(aq)}$ content from $HCl_{(aq)}$, $LiCl_{(aq)}$, and $NpCl_{4(aq)}$ and do not include $NaClO_{2(aq)}$ nor $NaClO_{2(aq)}$ disproportionation products.

aqueous solution that was dilute in $Np^{4+}_{(aq)}$ (1.6 mM, 1 μmol, 600 μL) and dilute in $HCl_{(aq)}$ (0.02 M). Analyses by UV-vis spectroscopy showed that the $Np^{4+}_{(aq)}$ reagent reacted immediately with $NaClO_{2(aq)}$. Then, the $Np^{4+}_{(aq)}$ and $NpO_2^{1+}_{(aq)}$ product-to-reagent ratio stabilized within 60 s. These experiments showed that reacting a small amount [more than two equivalents *vs.* $Np^{4+}_{(aq)}$] of $NaClO_{2(aq)}$ (2.2 μmol; 330 μL of a 7.2 mM solution) with one equivalent of $Np^{4+}_{(aq)}$ (1 μmol) generated a one-to-one mixture of $Np^{4+}_{(aq)}$ and $NpO_2^{1+}_{(aq)}$. Increasing the quantity of $NaClO_{2(aq)}$ increased the amount of $NpO_2^{1+}_{(aq)}$ generated until approximately 4.5 equivalents of $NaClO_{2(aq)}$ (4.5 μmol; 630 μL of 7.2 mM solution) *vs.* one equivalent of $Np^{4+}_{(aq)}$ (1 μmol) had been added. In this situation, the $Np^{4+}_{(aq)}$ reagent was completely consumed and $NpO_2^{1+}_{(aq)}$ formed. The $NpO_2^{1+}_{(aq)}$ species was stable under ambient conditions during a 5-day monitoring process.

The $Np^{4+}_{(aq)}$ cation also oxidized to $NpO_2^{1+}_{(aq)}$ when the $NaClO_{2(aq)}$ concentration was increased from 3.4 mM to 32 mM; entry 2 in Table 1. However, under these conditions the $NpO_2^{1+}_{(aq)}$ mono-cation was not stable with time and further oxidation to $NpO_2^{2+}_{(aq)}$ occurred (Fig. 5). Absorption peaks from $NpO_2^{1+}_{(aq)}$ at 10 400 cm^{-1} (980 nm) and 8700 cm^{-1} (1150 nm) were replaced within one hour by features characteristic of $NpO_2^{2+}_{(aq)}$; 7900 cm^{-1} (1270 nm). Monitoring this product by UV-vis spectroscopy revealed that $NpO_2^{2+}_{(aq)}$ was stable for at least 5 days, when monitoring ceased. Comparing this data with that presented above highlighted how formation of $NpO_2^{2+}_{(aq)}$ *vs.* $NpO_2^{1+}_{(aq)}$ could be controlled based on ingoing $NaClO_{2(aq)}$ concentrations. The $NpO_2^{1+}_{(aq)}$ mono-cation was generated when the ingoing concentration of $NaClO_{2(aq)}$ was low (3.4 mM; entry 1, Table 1). In contrast, the $NpO_2^{2+}_{(aq)}$
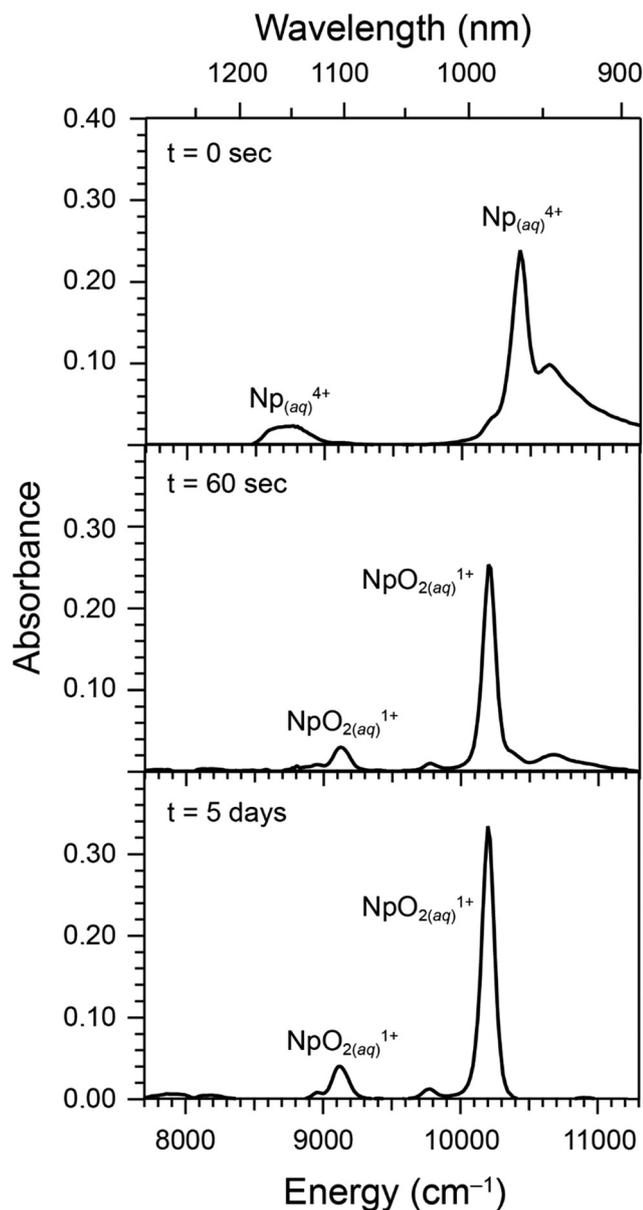
This journal is © The Royal Society of Chemistry and the Centre National de la Recherche Scientifique 2024

Fig. 2 UV-vis absorption spectra documenting oxidation of $Np^{4+}_{(aq)}$ to $NpO_2^{1+}_{(aq)}$ as a function of time (top, initial; middle, after 60 s; bottom, after 5 days). Entry #1 in Table 1 describe the reaction conditions. Ingoing concentrations were low for $Np^{4+}_{(aq)}$ (0.81 mM), low for $NaClO_{2(aq)}$ (3.4 mM), low for $H^{1+}_{(aq)}$ (0.02 M), and low for $Cl^{1-}_{(aq)}$ (0.026 M). Hence, the ingoing $HCl_{(aq)}$ concentration was 0.02 M and there no added $LiCl_{(aq)}$.

di-cation was generated with the ingoing concentration of $NaClO_2$ was high (32 mM; entry 2, Table 1). There is a disclaimer associated with this conclusion. Controlling oxidation of $Np^{4+}_{(aq)}$ to either $NpO_2^{1+}_{(aq)}$ or $NpO_2^{2+}_{(aq)}$ required the ingoing concentrations of $Np^{4+}_{(aq)}$ and $NaClO_{2(aq)}$ as well as ingoing concentrations of $Cl^{1-}_{(aq)}$ and $H^{1+}_{(aq)}$ to be carefully managed; see experiments captured in entries 2 to 19 in Table 1. For example, adding $NaClO_{2(aq)}$ (32 mM or 31 mM to 160 mM entries 2 to 5) to $Np^{4+}_{(aq)}$ (1.5 mM to 3.1 mM) with low $Cl^{1-}_{(aq)}$ and $H^{1+}_{(aq)}$ concentrations (0.02 to 0.04 M) generated $NpO_2^{1+}_{(aq)}$ at the 1 h timestamp and that $NpO_2^{1+}_{(aq)}$ converted

to $NpO_2^{2+}_{(aq)}$ within 24 h. Increasing the $Cl^{1-}_{(aq)}$ content changed this outcome. By using the $LiCl_{(aq)}$ to increase Cl^{1-} concentrations to >9 M (entries 6 to 9) and holding the H^{1+} concentration low (0.02 M to 0.04 M) stabilized the $Np^{4+}_{(aq)}$ regent as the dominant specie present in solution at the 1 h timestamp. Then, the $Np^{4+}_{(aq)}$ cation oxidized to $NpO_2^{2+}_{(aq)}$ within 24 h. Increasing both $H^{1+}_{(aq)}$ and Cl^{1-} content to >5.4 M shut down the oxidation of $Np^{4+}_{(aq)}$ to $NpO_2^{2+}_{(aq)}$ and $Np^{4+}_{(aq)}$ was stable throughout the 24 h monitoring duration.

We characterized the reaction rates for entry 2 in Table 1 that were associated with the transformation of (1st) $Np^{4+}_{(aq)}$ to $NpO_2^{1+}_{(aq)}$ and (2nd) $NpO_2^{1+}_{(aq)}$ to $NpO_2^{2+}_{(aq)}$ (Fig. 6). The oxidation of $Np^{4+}_{(aq)}$ to $NpO_2^{1+}_{(aq)}$ proceeded with fractional order dependence on both the $Np^{4+}_{(aq)}$ (0.300 ± 0.008) and $ClO_2^{1-}_{(aq)}$ (0.110 ± 0.002) reagents. The reaction rate law derived from the oxidation of $NpO_2^{1+}_{(aq)}$ to $NpO_2^{2+}_{(aq)}$ was approximately first order in $NpO_2^{1+}_{(aq)}$ (0.98 ± 0.02) and higher order (1.7 ± 0.01) with regards to $NaClO_{2(aq)}$. No evidence was obtained that suggested the $NpO_2^{2+}_{(aq)}$ di-cation formed *via* disproportionation of the $NpO_2^{1+}_{(aq)}$ mono-cation to $Np^{4+}_{(aq)}$ and $NpO_2^{2+}_{(aq)}$. For instance, regeneration of $Np^{4+}_{(aq)}$ – or a sustained presence of $Np^{4+}_{(aq)}$ – after initial formation of $NpO_2^{1+}_{(aq)}$ was not observed. Instead, our data suggested that $NpO_2^{1+}_{(aq)}$ converted directly to $NpO_2^{2+}_{(aq)}$. Admittedly, this data does not completely rule out the possibility of a low-concentration $Np^{4+}_{(aq)}$ transient intermediate nor the possibility of disproportionation reaction pathways. However, with the data in hand at this time, it seemed possible that $NpO_2^{1+}_{(aq)}$ was converted directly $NpO_2^{2+}_{(aq)}$ by the redox processes accessed with $NaClO_{2(aq)}$ and/or $NaClO_{2(aq)}$ decomposition productions, see eqn (1) and (2).

There were other experimental conditions that generated a $NpO_2^{1+}_{(aq)}$ intermediate (within an hour) that in turn oxidized $Np^{4+}_{(aq)}$ to $NpO_2^{2+}_{(aq)}$ (entries 3 to 10 from Table 1). Each of these scenarios had three commonalities: the ingoing $H^{1+}_{(aq)}$ concentrations ranged 0.02 to 5.4 M, the ingoing $Cl^{1-}_{(aq)}$ concentration ranged from 0.026 to 9.1 M, the ingoing $Np^{4+}_{(aq)}$ concentrations were larger than 0.81 mM (entries 2 through 5 in Table 1), and the ingoing $NaClO_{2(aq)}$ concentrations were high (>31 mM). Modifying these variables changed the reaction outcomes. For example, increasing $Cl^{1-}_{(aq)}$ content to >9 M – using $LiCl_{(aq)}$ – masked observation of a $NpO_2^{1+}_{(aq)}$ intermediate (entries 6 to 10 in Table 1; Fig. 7 and 8). In these situations, we only observed disappearance of $Np^{4+}_{(aq)}$ and formation of $NpO_2^{2+}_{(aq)}$ (entries 6 to 9). Monitoring this reaction as a function of time revealed that the loss of $Np^{4+}_{(aq)}$ and formation of $NpO_2^{2+}_{(aq)}$ proceeded at fourth order (4.11 ± 0.09) dependence with respect to $Np^{4+}_{(aq)}$ and fractional (0.50 ± 0.07) order with respect to $NaClO_{2(aq)}$ (Fig. 8). Although fourth order rate laws have been measured before,[64–67] we acknowledge their unusuality and rarity. In our case, we speculated that the measured fourth order rate law resulted from numerous intertwined reactions that were occurring simultaneously. One obvious possibility included $NaClO_{2(aq)}$ decomposition products reacting directly with $Np^{4+}_{(aq)}$ to generate $NpO_2^{2+}_{(aq)}$ and maybe a transient $NpO_2^{1+}_{(aq)}$ intermediate. It is also

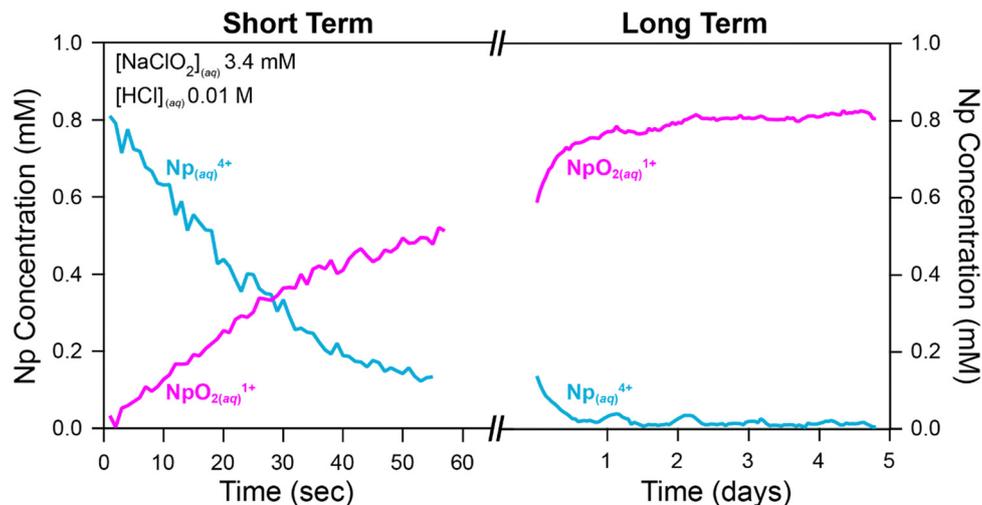**Fig. 3** Peak intensity from UV-vis spectra from $Np^{4+}_{(aq)}$ (teal trace from the absorption peak at 10 400 cm^{-1}, 960 nm) and $NpO_2^{1+}_{(aq)}$ (magenta trace from the absorption peak at 9100 cm^{-1}, 1100 nm) plotted as a function of two different time intervals (left, 0 to 1 min; right, 0.1 to 5 days). Entry #1 in Table 1 describe the reaction conditions. Ingoing concentrations were low for $Np^{4+}_{(aq)}$ (0.81 mM), low for $NaClO_2_{(aq)}$ (3.4 mM), low for $H^{1+}_{(aq)}$ (0.02 M), and low for $Cl^{1-}_{(aq)}$ (0.02 M). Hence, the ingoing $HCl_{(aq)}$ concentration was 0.02 M and there was no added LiCl.

Fig. 4 A plot showing how oxidation of $Np^{4+}_{(aq)}$ (teal trace from the absorption peak at 10 400 cm^{-1}, 960 nm) to $NpO_2^{1+}_{(aq)}$ (magenta trace from the absorption peak at 10 200 cm^{-1}, 980 nm) depended on the amount of added $NaClO_2_{(aq)}$. Ingoing concentrations were low for $Np^{4+}_{(aq)}$ (1.6 mM), low for $H^{1+}_{(aq)}$ (0.02 M), and low for $Cl^{1-}_{(aq)}$ (0.026 M). Hence, the ingoing $HCl_{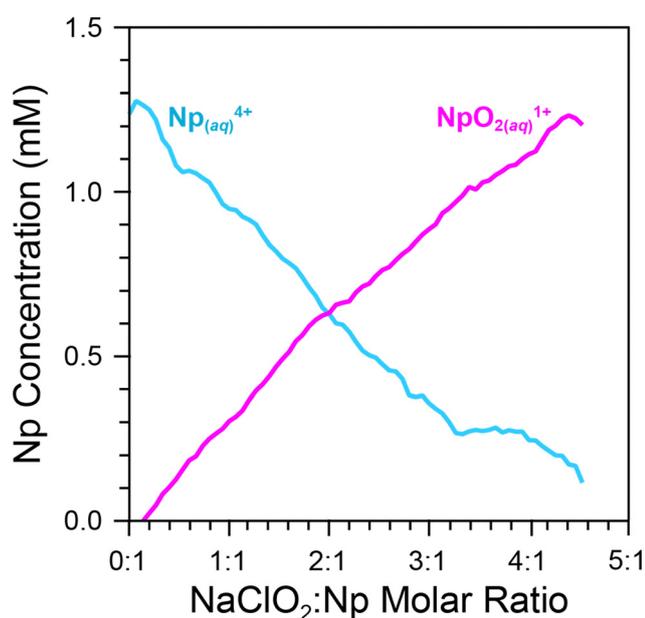(aq)}$ concentration was 0.02 M and there was no added LiCl. The $NaClO_2_{(aq)}$ started at zero and increased with addition of 10 µL aliquots of a $NaClO_2_{(aq)}$ (7.2 mM) solution. Concentrations were corrected for dilutions.

Fig. 5 Top: UV-vis absorption spectra documenting oxidation of $Np^{4+}_{(aq)}$ (teal trace) to $NpO_2^{1+}_{(aq)}$ (magenta trace) as a function of time (2 min). Bottom: Subsequent oxidation of $NpO_2^{1+}_{(aq)}$ (magenta trace) to $NpO_2^{2+}_{(aq)}$ (black trace). Entry #2 in Table 1 describe the reaction conditions. Ingoing concentrations were low for $Np^{4+}_{(aq)}$ (1.5 mM), low for $NaClO_2_{(aq)}$ (32 mM), low for $H^{1+}_{(aq)}$ (0.02 M), and low for $Cl^{1-}_{(aq)}$ (0.02 M). Hence, the ingoing $HCl_{(aq)}$ concentration was 0.02 M and there was no added LiCl.

possible that the $NaClO_2_{(aq)}$ could react with $Np^{4+}_{(aq)}$ directly. If any $NpO_2^{1+}_{(aq)}$ formed, that mono-cation could disproportionate to generate $NpO_2^{2+}_{(aq)}$ and regenerate $Np^{4+}_{(aq)}$. Note, we did not detect evidence for formation of a $Np^{4+}_{(aq)}$ intermediate by UV-vis. Hence, if $Np^{4+}_{(aq)}$ formed, it was generated in relatively small quantities.

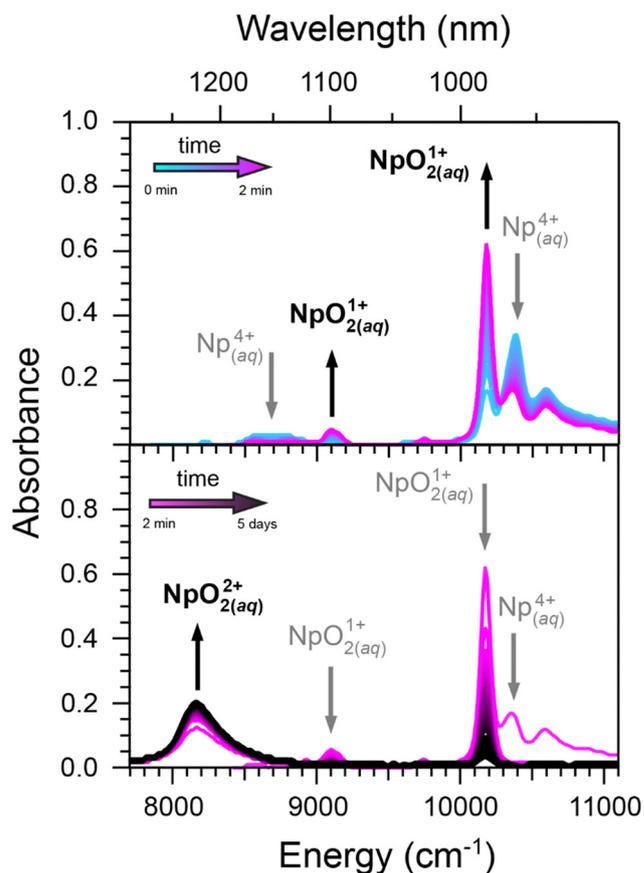**Fig. 6** Peak intensity from UV-vis spectra from $Np^{4+}_{(aq)}$ (teal trace at 10 400 cm^{-1}, 960 nm), $NpO_2^{1+}_{(aq)}$ (magenta trace at 9100 cm^{-1}, 1100 nm), and $NpO_2^{2+}_{(aq)}$ (black trace at 8200 cm^{-1}, 1250 nm) plotted as a function of two different time intervals (left, 0 to 2 min; right, approximately 2 min to 10 days). Entry #5 in Table 1 describe the reaction conditions. Ingoing concentrations were high for $Np^{4+}_{(aq)}$ (3.1 mM), high for $NaClO_{2(aq)}$ (160 mM), low for $H^{1+}_{(aq)}$ (0.04 M), and low for $Cl^{1-}_{(aq)}$ (0.052 M). Hence, the ingoing $HCl_{(aq)}$ concentration was 0.04 M and there was no added LiCl.

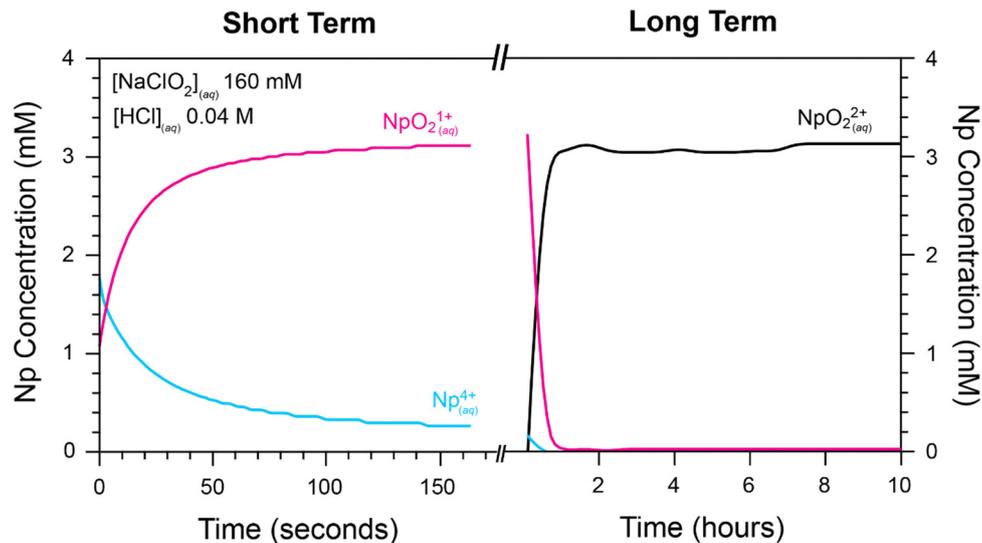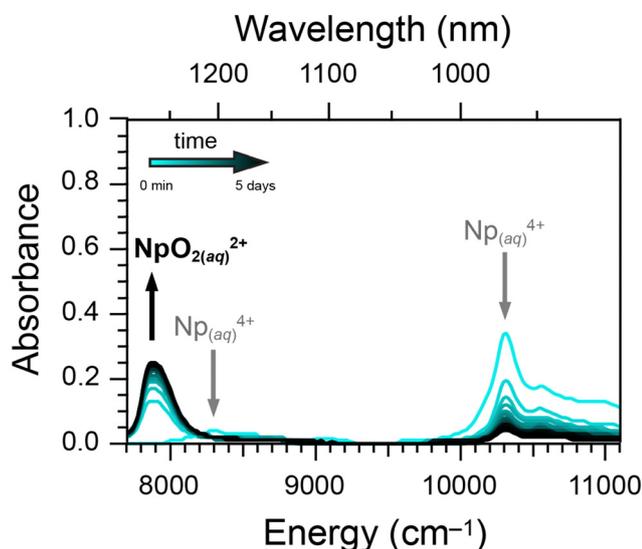**Fig. 7** UV-vis absorption spectra documenting oxidation of $Np^{4+}_{(aq)}$ (teal trace) to $NpO_2^{2+}_{(aq)}$ (black trace). Entry #7 in Table 1 describe the reaction conditions. Ingoing concentrations were 1.5 mM for $Np^{4+}_{(aq)}$, 32 mM for $NaClO_{2(aq)}$, 0.02 M for $H^{1+}_{(aq)}$, and 9.2 M for $Cl^{1-}_{(aq)}$. Hence the ingoing $HCl_{(aq)}$ concentration was 0.02 M and for $LiCl_{(aq)}$ was 9.2 M.

Regardless, we are intrigued by this reaction and our current efforts are focused on better characterizing how $NaClO_{2(aq)}$ incites $Np^{4+}_{(aq)}$ transformation to $NpO_2^{2+}_{(aq)}$ in high $Cl^{1-}_{(aq)}$ solutions.

As shown in Table 1 (entries 11 to 19), oxidation of $Np^{4+}_{(aq)}$ to $NpO_2^{2+}_{(aq)}$ was halted when the $H^{1+}_{(aq)}$ and $Cl^{1-}_{(aq)}$ concentrations were $\geq$5.4 M, when the ingoing $Np^{4+}_{(aq)}$ concentration ranged 1.5 to 2.9 mM, and the $NaClO_{2(aq)}$ concentration was high (31 to 160 mM). It is particularly important to highlight these observations because of their relevance to EXCEL processing

methods described in the introduction. Notice, that the $NaClO_{2(aq)}$ redox agent held neptunium in the +4 oxidation state under conditions that mimicked plutonium processing by EXCEL: when the $H^{1+}_{(aq)}$ and $Cl^{1-}_{(aq)}$ concentrations were >5.4 M and the $NaClO_{2(aq)}$ concentrations varied from 31 mM to 160 mM, and $Np^{4+}_{(aq)}$ concentrations varied from 1.5 mM to 2.9 mM (entries 11 to 19 in Table 1). This data suggested that – all things being equal – neptunium should follow plutonium through within the EXCEL processing steps.

Molar extinction coefficients

Table 2 compares molar extinction coefficients (ε) for neptunium absorption peaks calculated for experimental conditions described in Table 1 when Np was in a single oxidation state. These data were important for quantifying $Np^{4+}_{(aq)}$, $NpO_2^{1+}_{(aq)}$, and NpO_2^{2+} abundance in the reactions studied herein and provided insight into the solution phase behavior of $Np^{4+}_{(aq)}$ and $NpO_2^{2+}_{(aq)}$. In terms of the latter topic, we observed that ε for the $Np^{4+}_{(aq)}$ absorption feature at 10 400 cm^{-1} (960 nm) decreased with increasing $Cl^{1-}_{(aq)}$ concentration. In addition, increasing $Cl^{1-}_{(aq)}$ shifted the $Np^{4+}_{(aq)}$ absorption peaks lower in energy (Fig. 9). These absorption changes are often associated with increased $Cl^{1-}_{(aq)}$ complexation of neptunium.[36,37,68] It was interesting to note that ε for the $Np^{4+}_{(aq)}$ peak at 8700 cm^{-1} (1150 nm) peak was shifted in energy but the ε value was unaffected by changes in $Cl^{1-}_{(aq)}$ content (see Fig. 9). For $NpO_2^{2+}_{(aq)}$, increasing the $Cl^{1-}_{(aq)}$ caused the absorption feature at 8200 cm^{-1} (1220 nm) to decrease in energy and shift higher in energy, which is also often attributed to increased $Cl^{1-}_{(aq)}$ complexation.[69] Another intriguing observation was that ε for the 10 400 cm^{-1} absorbance peak from $Np^{4+}_{(aq)}$ was more impacted by $Cl^{1-}_{(aq)}$ concentrations than those from $NpO_2^{2+}_{(aq)}$ at 8200 cm^{-1}. This stronger depended of ε on $Cl^{1-}_{(aq)}$ concentration tracked with the Lewis acidity for the $Np^{4+}_{(aq)}$ *vs.*
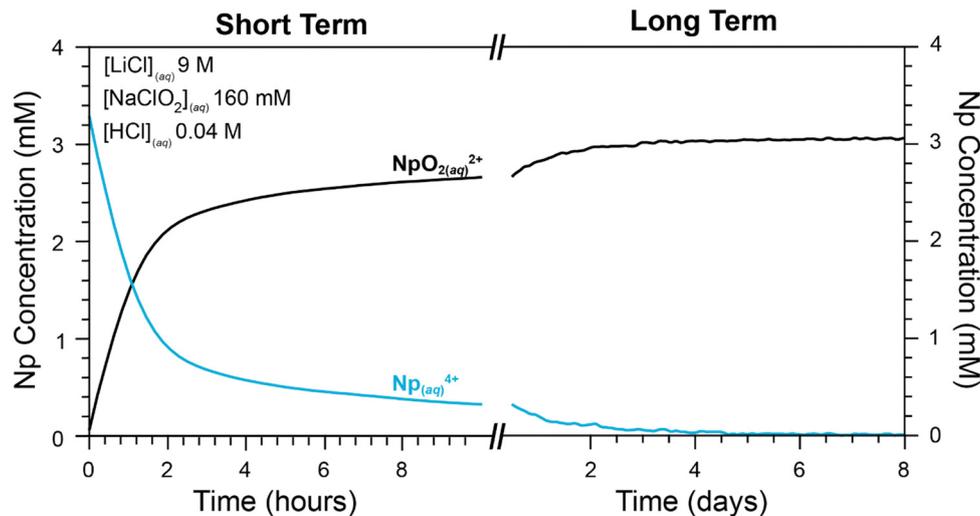
Fig. 8 Peak intensity from UV-vis spectra from $Np^{4+}_{(aq)}$ (teal trace at 10 400 cm^{-1}, 960 nm) and $NpO_2^{2+}_{(aq)}$ (black trace at 7900 cm^{-1}, 1270 nm) plotted as a function of two different time intervals (left, 0 to 2 min; right, 2 min to 10 days). Entry #9 in Table 1 describe the reaction conditions. Ingoing concentrations were high for $Np^{4+}_{(aq)}$ (3.1 mM), high for $NaClO_{2(aq)}$ (160 mM), low for $H^{1+}_{(aq)}$ (0.04 M), and high for $Cl^{1-}_{(aq)}$ (9.1 M). Hence, the ingoing $HCl_{(aq)}$ concentration was 0.04 M and for $LiCl_{(aq)}$ was 9.1 M.

Table 2 Molar extinction coefficients (ε) obtained for neptunium species present in aqueous solutions under the experimental conditions specified below

Oxidation state	Energy (cm^{-1})	Wavelength (nm)	Table 1 entry #	ε (M^{-1} cm^{-1})
$Np^{4+}_{(aq)}$	10 400	960	1	294
$Np^{4+}_{(aq)}$	10 400	960	3	304
$Np^{4+}_{(aq)}$	10 400	960	2	341
$Np^{4+}_{(aq)}$	10 400	960	7	220
$Np^{4+}_{(aq)}$	10 400	960	6	171
$Np^{4+}_{(aq)}$	10 400	960	N/A	162[a]
$Np^{4+}_{(aq)}$	8700	1150	2	19
$Np^{4+}_{(aq)}$	8700	1150	3	20
$Np^{4+}_{(aq)}$	8700	1150	7	26
$Np^{4+}_{(aq)}$	8700	1150	6	20
$NpO_2^{1+}_{(aq)}$	10 200	980	1	334
$NpO_2^{1+}_{(aq)}$	10 200	980	3	660
$NpO_2^{1+}_{(aq)}$	10 200	980	4	790
$NpO_2^{1+}_{(aq)}$	10 200	980	5	446
$NpO_2^{1+}_{(aq)}$	10 200	980	N/A	375[a]
$NpO_2^{1+}_{(aq)}$	9100	1100	1	41
$NpO_2^{1+}_{(aq)}$	9100	1100	3	53
$NpO_2^{1+}_{(aq)}$	9100	1100	4	60
$NpO_2^{1+}_{(aq)}$	9100	1100	5	50
$NpO_2^{2+}_{(aq)}$	8200	1220	4	127
$NpO_2^{2+}_{(aq)}$	8200	1220	5	115
$NpO_2^{2+}_{(aq)}$	8200	1220	N/A	43[a]
$NpO_2^{2+}_{(aq)}$	7900	1270	8	190
$NpO_2^{2+}_{(aq)}$	7900	1270	7	190
$NpO_2^{2+}_{(aq)}$	7900	1270	9	174

[a] In 2 M $HClO_{4(aq)}$ from ref. 37.

$NpO_2^{2+}_{(aq)}$ cations as well as the variances in $Cl^{1-}_{(aq)}$ complexation constants.[37,70]

Outlook

Herein, we observed that $NaClO_{2(aq)}$ enabled $Np^{4+}_{(aq)}$ to access many redox events in acidic aqueous solutions (Scheme 1).

Moreover, oxidation product identities could be controlled as a function of time by manipulating four variables; ingoing concentrations of (1) $Np^{4+}_{(aq)}$, (2) $NaClO_{2(aq)}$, (3) $Cl^{1-}_{(aq)}$, and (4) $H^{1+}_{(aq)}$. For example, $NpO_2^{1+}_{(aq)}$ exclusively formed when $Np^{4+}_{(aq)}$, $NaClO_{2(aq)}$, $Cl^{1-}_{(aq)}$, and $H^{1+}_{(aq)}$ concentrations were all relatively low. Increasing the $Cl^{1-}_{(aq)}$ concentration and/or increasing the $NaClO_{2(aq)}$ concentration generated $NpO_2^{2+}_{(aq)}$, provided that the $H^{1+}_{(aq)}$ concentration was also low. Finally, $Np^{4+}_{(aq)}$ was stabilized when the $H^{1+}_{(aq)}$ and $Cl^{1-}_{(aq)}$ concentrations were high (> 5.4 M), regardless of the ingoing $NaClO_{2(aq)}$ and $Np^{4+}_{(aq)}$ concentrations.

Regarding applications for plutonium processing methods described in the introduction, we make the following prediction. Our data suggested that the neptunium oxidation state during plutonium processing will be either maintained at +4 or a mixture of +4 and +6 if plutonium separations are carried out at high $NaClO_{2(aq)}$, high $Cl^{1-}_{(aq)}$, high $H^{1+}_{(aq)}$, and low $Np^{4+}_{(aq)}$ concentrations. If we are correct, the $^{237}Np_{(aq)}$ contaminant will follow $Pu^{4+}_{(aq)}$ through processing lines. However, we acknowledge that there are substantial differences between the fundamental studies carried out here *vs.* real-world processing environments (*e.g.* radiation effects, scaling effects from other impurities, *etc.*). To improve relevancy, future work will center on understanding how other constituents present in various plutonium and americium waste streams impact redox chemistry between $^{237}Np_{(aq)}$ and $NaClO_{2(aq)}$.

The data in Table 1 and Scheme 1 also demonstrated that the neptunium, $NaClO_{2(aq)}$, $H^{1+}_{(aq)}$, and $Cl^{1-}_{(aq)}$ concentration variables were intertwined and must be delicately managed to control the $Np^{4+}_{(aq)}$ oxidation to $NpO_2^{1+}_{(aq)}$ *vs.* $NpO_2^{2+}_{(aq)}$ by way of $NaClO_{2(aq)}$. These studies provided a more sophisticated understanding of aqueous actinide electron transfer chemistry and offer opportunity to better predict and control actinide redox processes. Future efforts will center on developing a
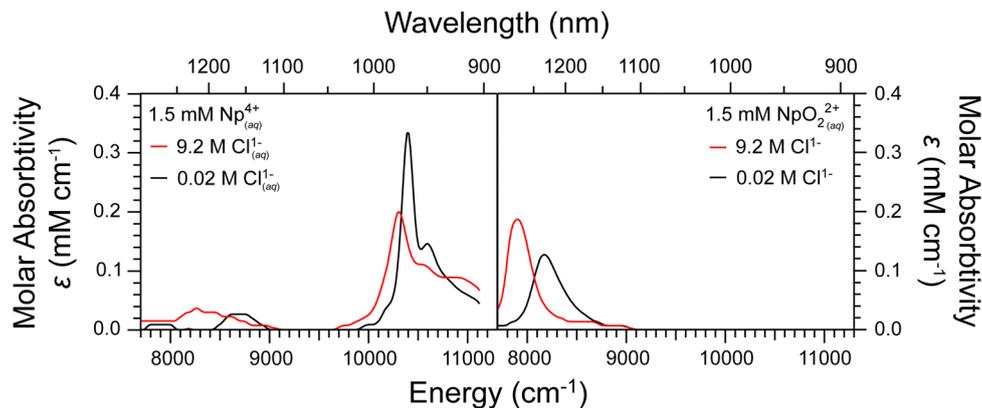
Fig. 9 UV-vis absorption spectra documenting oxidation of the $Np^{4+}_{(aq)}$ reagent (left) to the $NpO_2^{1+}_{(aq)}$ product (right) from entries #4 (black trace) and #8 (red trace). This figure highlights how moving from low concentration Cl^{1-} (0.026 M; entry #4, black trace) to high concentration Cl^{1-} (9.2 M, entry #8, red trace) impacts the absorption features. Note, other than Cl^{1-} concentration, the other experimental variables were held constant between these two experiments. Ingoing concentrations associated with the entry #4 (black trace) experiment were 1.5 mM for $Np^{4+}_{(aq)}$, 160 mM for $NaClO_{2(aq)}$, 0.02 M for $H^{1+}_{(aq)}$, and 0.026 M for $Cl^{1-}_{(aq)}$. In this case, the ingoing $HCl_{(aq)}$ concentration was 0.02 M and there was no LiCl added. Ingoing concentrations associated with the entry #8 (red trace) experiment were 1.5 mM for $Np^{4+}_{(aq)}$, 160 mM for $NaClO_{2(aq)}$, 0.02 M for $H^{1+}_{(aq)}$, and 9.2 M for $Cl^{1-}_{(aq)}$.

better understanding on what reaction pathways are responsible for the oxidation of $Np^{4+}_{(aq)}$ by $NaClO_{2(aq)}$. On an applied level, these types of studies – alongside the data reported herein – will impact waste stewardship programs, production of pure isotopes, and touch on many processing campaigns associated with actinide reliant technologies.

Methods

General considerations

¡*CAUTION!* Neptunium-237 $[^{237}Np, t_{1/2} = 2.144(6) \times 10^6 \, y]^{33}$ and its daughter products constitute serious health threats because of radioactive decay. Hence, all experiments that involved manipulation of these radionuclides were conducted in a radiological buffer area that contained HEPA filtered hoods, continuous air monitors, negative pressure gloveboxes, and monitoring equipment appropriate for α-, β-, and γ-particle detection. Entrance into the laboratory space was controlled with a hand and foot monitoring instrument for α-, β-, and γ-emitting isotopes and a full body personal contamination monitoring station.

Aqueous hydrochloric acid [$HCl_{(aq)}$, Fisher Scientific, Optima® grade] and sodium chlorite ($NaClO_2$, 80%, Sigma Aldrich) was obtained commercially and used as received. Water (H_2O) was deionized, passed through a Barnstead water purification system to achieve resistivity of 18 MΩ cm, and purified further *via* distillation using a Teflon distillation apparatus. Chemically pure and oxidation state pure stock solutions of $Np^{4+}_{(aq)}$ were obtained from ^{237}Np samples that had been recovered from previous experimental campaigns, as described previously.[59] In general, these ^{237}Np samples were combined and processed using a series of precipitations, valence adjustments, and ion exchange chromatography. The end result was a chemically pure, emerald green stock solution that contained $Np^{4+}_{(aq)}$ (66 mM) in $HCl_{(aq)}$ (1 M).[59]

UV-Vis spectroscopy

All UV-vis spectroscopy measurements were conducted using a Stellar Net EXtended Range NIR Spectrometer and/or Ocean Insight NIR Quest Spectrometer. To mitigate hazards associated with making optical measurements on radioactive samples, the cuvette holder was housed within a HEPA filtered chemical fume hood. This holder was connected to the UV-vis spectrometer using fiber optics and the neptunium samples were contained within the fume hood in screw top quartz cuvettes (Starna Scientific). Neptunium concentrations were determined by monitoring the following absorption peaks: 10 400 cm^{-1} (960 nm) and/or 8700 cm^{-1} (1150 nm) for $Np^{4+}_{(aq)}$, 10 200 cm^{-1} (980 nm) and/or 9100 cm^{-1} (1100 nm) for $NpO_2^{1+}_{(aq)}$, 8200 cm^{-1} (1220 nm) and/or 7900 cm^{-1} (1270 nm) for $NpO_2^{2+}_{(aq)}$.

Data acquisition and analysis

Before handling the Np stock, a reference UV-vis spectra was initially obtained from pure $HCl_{(aq)}$ (0, 6, 7, or 8 M) or $LiCl_{(aq)}$ (10 M) solutions prior to assaying $Np^{4+}_{(aq)}$ and $NaClO_{2(aq)}$ containing solutions. Data from $Np^{4+}_{(aq)}$ and $NaClO_{2(aq)}$ reactions were background subtracted by setting the intensity at 9520 cm^{-1} (1050 nm) to zero. Reaction rate constants were determined using the systematic numerical procedure by which the concentration of one variable was varied (*e.g.* ingoing $Np^{4+}_{(aq)}$) whilst the other three variables were held constant [in this scenario, ingoing $NaClO_{2(aq)}$, $H^{1+}_{(aq)}$, and $Cl^{1-}_{(aq)}$].[71,72] The linear initial reaction rate was taken to be the rate by which $Np^{4+}_{(aq)}$ reacted (after mixing) by using linear regression. Errors for the analysis of reactions rates were calculated through propagation of error in measurements of ingoing $NaClO_{2(aq)}$ mass, pipetting, and volumetric flasks. An example calculation may be found in the ESI.† Molar extinction coefficients were calculated using the Beer–Lambert Law.[73]

Using dilute aqueous sodium chlorite solutions, NaClO$_{2(aq)}$, to generate oxidation state pure solutions of neptunyl(v), NpO$_2^{1+}$$_{(aq)}$

In a fume hood and with no attempt to exclude air and moisture, an aliquot (15 μL; 0.2 mg, 1 μmol of Np^{4+}) of the aforementioned Np^{4+}$_{(aq)}$ stock solution (66 mM Np^{4+}) in HCl$_{(aq)}$ (1 M) was added to a screw-top quartz cuvette charged with H$_2$O (600 μL). The Np^{4+}$_{(aq)}$ concentration for this new 615 μL solution was now 1.6 mM. Meanwhile, in a separate beaker, a dilute solution of NaClO$_{2(aq)}$ (6.9 mM) was prepared by dissolving NaClO$_{2(s)}$ (0.0389 g, 80%, 0.344 mmol) in H$_2$O (50 mL). An aliquot (600 μL, 4 μmol) from this NaClO$_{2(aq)}$ solution was added all at once to the Np^{4+}$_{(aq)}$ containing cuvette. ¡CAUTION! The combination of HCl$_{(aq)}$ and NaClO$_{2(aq)}$ is vigorous, can bubble, and generates toxic gases (like ClO$_2$). To mitigate these hazards, we implemented the following engineering and administrative controls. First, the aliquot of the NaClO$_{2(aq)}$ was added slowly (over the course of 5 seconds to the Np^{4+}$_{(aq)}$ containing cuvette). Second, the manipulation was carried out in a chemical fume hood, behind glass shielding, to guard the worker from evolved gases. Third, secondary containment was used to avoid spreading ^{237}Np-contamination, which can result from potential splattering. Finally, the screw top cuvette was only loosely capped, to avoid pressurization. The reagents were mixed by pumping the solution (from bottom to top) with a transfer pipette at least 4 times. This mixing action marked zero time for the reaction. It is relevant to note that the concentrations at the zero time for this solution (1.2 mL) were 0.81 mM for Np$_{(aq)}$, 3.4 mM for NaClO$_{2(aq)}$, and 0.01 M for HCl$_{(aq)}$. The cuvette was inserted into the UV-vis holder, the apparatus covered (to exclude ambient light), and the spectra were collected repeatedly over the course of a 5-day monitoring process.

Using concentrated aqueous sodium chlorite solutions, NaClO$_{2(aq)}$, to generate oxidation state pure solutions of neptunyl(vi), NpO$_2^{2+}$$_{(aq)}$

In a fume hood and with no attempt to exclude air and moisture, oxidation state pure solutions of NpO$_2^{2+}$$_{(aq)}$ were prepared using an adaptation of the procedure described in the preceding section titled, "Using Dilute Aqueous Sodium Chlorite Solutions, NaClO$_{2(aq)}$, to Generate Oxidation State Pure Solutions of Neptunyl(v)." The major difference between these procedures was associated with the amount of added NaClO$_{2(aq)}$ used to oxidize Np^{4+}$_{(aq)}$. Toward this end, a more concentrated solution of NaClO$_{2(aq)}$ (2.6 M) was prepared by dissolving NaClO$_{2(s)}$ (298 mg, 2.6 mmol) in H$_2$O (1 mL). Then, the NaClO$_{2(aq)}$ (40 μL, 2.6 M, 104 μmol) and Np^{4+}$_{(aq)}$ (615 μL, 1.6 mM, 1 μmol) solutions were combined in a cuvette. **CAUTION!** *See precautions described above that were implemented to mitigate this hazardous combination activity.* The reagents were mixed by pumping the solution (from bottom to top) with a transfer pipette at least 4 times. This mixing action marked zero time for the reaction. The reagent concentrations at the zero time for this solution (655 μL) were 1.5 mM for Np^{4+}$_{(aq)}$, 160 mM for NaClO$_{2(aq)}$ (approximate), and 0.02 M for HCl$_{(aq)}$. The cuvette

was inserted into the UV-vis holder, the apparatus covered (to exclude ambient light), and the spectra were collected repeatedly over the course of a 5 day monitoring period.

Evaluating how four variables impacted oxidation of neptunium by sodium chlorite; Np^{4+}$_{(aq)}$ + NaClO$_{2(aq)}$

In a fume hood and with no attempt to exclude air and moisture, oxidation of Np^{4+}$_{(aq)}$ by NaClO$_{2(aq)}$ was investigated in HCl as a function of the following four variables, (1) Np^{4+}$_{(aq)}$ reagent concentration, (2) NaClO$_{2(aq)}$ oxidant concentration, (3) Cl^{1-}$_{(aq)}$ complexant concentration, and (4) H^{1+}$_{(aq)}$ concentration. This was achieved by modifying the experimental conditions described above in the antecedent section titled, "Using Dilute Aqueous Sodium Chlorite Solutions, NaClO$_{2(aq)}$, to Generate Oxidation State Pure Solutions of Neptunyl(v)." See Table 1 for a summary of those tested parameters and the primary neptunium oxidation states that formed within 1 h and within 24 h. These solutions were prepared by modifying the concentration of the ingoing reagents, oxidant, complexing agents, and acid. The ingoing Np^{4+}$_{(aq)}$ concentration was varied (1) by combining 15 μL of the Np^{4+}$_{(aq)}$ (66 mM) stock solution with the other reagents in a cuvette to generate a final solution that was dilute in Np^{4+}$_{(aq)}$ (1.5 mM) or (2) by combining 30 μL of the Np^{4+}$_{(aq)}$ (66 mM) stock solution with the other regents in a cuvette to generate a final solution that was highly concentrated in Np^{4+}$_{(aq)}$ (3.1 mM). The ingoing NaClO$_{2(aq)}$ concentration was varied (1) by combining 40 μL of a NaClO$_{2(aq)}$ (520 mM) stock solution with the other reagents in a cuvette to generate a final solution that was intermediately concentrated in NaClO$_{2(aq)}$ (31 or 32 mM) or (2) by combining 40 μL of a NaClO$_{2(aq)}$ (2.6 M) stock solution with the other reagents in a cuvette to generate a final solution that was highly concentrated in NaClO$_{2(aq)}$ (160 mM). The ingoing HCl$_{(aq)}$ concentration was varied (1) by combining either 600 μL of an HCl$_{(aq)}$ (6 to 8 M) stock solution with the other reagents in a cuvette to generate a final solution that was more concentrated in HCl$_{(aq)}$ (5.3 to 7.1 M) or (2) by adding an aliquot (15 or 30 μL, described above) from the neptunium stock solution [1 M HCl$_{(aq)}$] to a cuvette containing Teflon distilled H$_2$O (600 μL). This gave final volumes and concentrations of either 615 μL at 0.02 M HCl$_{(aq)}$ or 630 μL at 0.05 M HCl$_{(aq)}$. Then, NaClO$_{2(aq)}$ was added. These dilute HCl$_{(aq)}$ solutions also served as low ionic strength solutions, relatively speaking. High ionic strength solutions were prepared by combining 600 μL of a LiCl$_{(aq)}$ (10 M) stock solution with the other reagents in a cuvette to generate a final solution that was 9.0 to 9.2 M in LiCl$_{(aq)}$.

Conflicts of interest

There are no conflicts to declare.

Acknowledgements

References

1 P. Paviet-Hartmann, C. Riddle, K. Campbell and E. Mausolf, *Overview of Reductants Utilized in Nuclear Fuel Reprocessing/Recycling, Report INL/CON-12-28006*, Idaho National Labs, Idaho Falls, Idaho, 2013.

2 B. J. Mincher, L. R. Martin and N. C. Schmitt, *Inorg. Chem.*, 2008, **47**, 6984–6989.

3 Z. Karoutas, J. Brown, A. Atwood, L. Hallstadius, E. Lahoda, S. Ray and J. Bradfute, *Prog. Nucl. Energy*, 2018, **102**, 68–78.

4 T. Allen, J. Busby, M. Meyer and D. Petti, *Mater. Today*, 2010, **13**, 14–23.

5 W. H. E. Schwarz, N. M. Shavaleev, S. N. Kalmykov, A. Y. Romanchuk and I. E. Vlasova, *Front. Chem.*, 2020, **1**, 630.

6 B. J. Mincher, G. Modolo and S. P. Mezyk, *Solvent Extr. Ion Exch.*, 2009, **27**, 1–25.

7 P. Baron, S. M. Cornet, E. D. Collins, G. DeAngelis, G. Del Cul, Y. Fedorov, J. P. Glatz, V. Ignatiev, T. Inoue, A. Khaperskaya, I. T. Kim, M. Kormilitsyn, T. Koyama, J. D. Law, H. S. Lee, K. Minato, Y. Morita, J. Uhlíř, D. Warin and R. J. Taylor, *Prog. Nucl. Energy*, 2019, 117.

8 J. E. Birkett, M. J. Carrott, O. Danny, C. J. Jones, C. J. Maher, C. V. Roube, R. J. Taylor and D. A. Woodhead, *J. Nucl. Sci. Technol.*, 2007, **44**, 337–343.

9 R. C. Thompson, *Radiat. Res.*, 1982, **90**, 1–32.

10 D. L. Clark, G. D. Jarvinen, C. Kowalczyk, J. Rubin and M. A. Stroud, *Actinide Research Quarterly: Plutonium Processing at Los Alamos, LALP-08-004*, Los Alamos National Labs, Los Alamos, New Mexico, 2008.

11 B. C. Reed, *The history and science of the Manhattan Project*, Springer, New York, 2014.

12 T. Feder, *Phys. Today*, 2015, **68**, 22–24.

13 S. K. Cary, K. S. Boland, J. N. Cross, S. A. Kozimor and B. L. Scott, *Polyhedron*, 2017, **126**, 220–226.

14 A. E. Waltar, *Encyclopedia of Nuclear Energy*, Elsevier, 2021, vol. 4, pp. 451–464.

15 C. Adam, N. Olga and L. Duane, *Final Radiological Assessment of External Exposure for CLEAR-Line Americium Recovery Operations, LA-UR-13-28160*, Los Alamos National Labs, Los Alamos, NM, 2014.

16 G. F. Vandegrift, *Sep. Sci. Technol.*, 2006, **23**, 1409–1421.

17 E. P. Horwitz, H. Diamond and K. A. Martin, *Solvent Extr. Ion Exch.*, 2007, **6299**, 447–470.

18 R. E. Isaacson and B. F. Judson, *Neptunium Recovery and Purification at Hanford, HW-SA-3283*, Hanford Site, Hanford, Washington, 1963.

19 H. E. Henry, D. G. Karraker and C. S. Schlea, *Neptunium Behavior in Solvent Extraction of Uranium at Savannah River Plant, DP-638*, Savanah River National Labs, Aiken, South Carolina, 1961.

20 M. Barr, L. Schulte, G. Jarvinen, J. Espinoza, T. Ricketts, Y. Valdez, K. Abney and R. Bartsch, *J. Radioanal. Nucl. Chem.*, 2001, **248**, 457–465.

21 R. A. Barr, M. E. Jarvinen, G. D. Schulte, L. D. Stark, P. C. Chamberlin, R. M. Abney, K. D. Ricketts, T. E. Valdez and Y. E. Bartsch, *Americium Separations from High Salt Solutions, LA-13676-MS*, Los Alamos National Labs, Los Alamos, New Mexico, 2000.

22 A. C. 74 and M. E. Killion, Proceedings of the 55th Conference: American Nuclear Society winter meeting, Los Angeles, CA, USA, 1987.

23 J. A. Schramke, E. F. U. Santillan and R. T. Peake, *Appl. Geochem.*, 2020, **116**, 104561.

24 B. T. Arko, D. Dan, S. L. Adelman, D. L. Huber, D. B. Kimball, S. A. Kozimor, M. N. Lam, V. Mocko, J. C. Shafer, B. W. Stein and S. L. Thiemann, *Ind. Eng. Chem. Res.*, 2021, **60**, 14282–14296.

25 B. T. Arko, D. Dan, S. Adelman, D. B. Kimball, S. A. Kozimor, M. M. Martinez, T. Mastren, D. L. Huber, V. Mocko, J. Rim, J. C. Shafer and W. Stein, *Mater. Adv.*, 2023, 265–283.

26 L. D. Schulte, J. R. FitzPatrick, R. R. Salazar, B. S. Schake and B. T. Martinez, *Sep. Sci. Technol.*, 1995, **30**, 1833–1847.

27 D. Christensen and P. Cunningham, *Los Alamos National Laboratory Qualifications For Lead Laboratory in Plutonium Pit Technology, LA-UR-92-1729*, Los Alamos National Labs, Los Alamos, New Mexico, 1992.

28 K. S. Gardner, D. B. Kimball and B. E. Skidmore, *Aqueous Chloride Operations Overview: Plutonium and Americium Purification/Recovery, LA-UR-16-27346*, Los Alamos National Labs, Los Alamos, NM, 2016.

29 W. H. Smith, *Evaluation of Chloride-Ion-Specific Electrodes as in situ Chemical Sensors for Monitoring Total Chloride Concentration in Aqueous Solutions Generated During the Recovery of Plutonium from Molten Salts Used in Plutonium Electrorefining Operations, LA—122461992*, Los Alamos National Labs, Los Alamos, New Mexico, 1992.

30 Nuclear Posture Review Report, US Department of Defense, Washington, DC, 2010.

31 B. Roberts, *Wash Q*, 2021, **44**, 123–142.

32 K. Reif, *Arms Control Today*, 2018, **48**, 29–30.

33 National Nuclear Data Center, **https://www.nndc.bnl.gov/nudat2/**, (accessed 21 April 2021).

34 L. R. Morss, N. M. Edelstein and J. Fuger, *The Chemistry of the Actinide and Transactinide Elements*, Springer, Dordrecht, The Netherlands, 3rd edn, 2006.

35 T. Hindman, J. C. Magnusson and L. B. LaChapelle, *J. Am. Chem. Soc.*, 1949, **71**, 687–693.

36 J. R. Yoshida, Z. Johnson, S. G. Kimura and T. Krsul, in *The Chemistry of the Actinide and Transactinide Elements*, ed.

L. R. Morss, N. M. Edelstein, and J. Fuger, Springer, Dordrecht, The Netherlands, 3rd edn, 2008, vol. 2 ch. 6, pp. 699–812.

37 G. A. Burney and R. M. Harbour, *Radiochemistry of Neptunium, NAS-NS-3060*, Savanah River National Labs, Aiken, South Carolina, 1974.

38 R. C. Thompson, *Radiat. Res.*, 1982, **90**, 1–32.

39 R. McConn Jr, C. Gesh, R. Pagh, R. Rucker and R. G. Williams III, *Compendium of Material Composition Data for Radiation Transport Modeling, PIET-43741-TM-963 PNNL-15870 Rev. 1*, Pacific Northwest National Lab, Richland, Washington, 2011.

40 T. Fukasawa, C. Lierse and J. I. Kim, *J. Nucl. Sci. Technol.*, 1996, **33**, 486–491.

41 B. R. Deshwal, H. D. Jo and H. K. Lee, *Can. J. Chem. Eng.*, 2004, **82**, 619–623.

42 G. Gordon in *Progress in Inorganic Chemistry*, ed. S. J. Lippard, Wiley, New York, 1972, vol. 15 ch. 3, pp. 201–286.

43 G. Holst, *Ind. Eng. Chem.*, 1950, **42**, 2359–2371.

44 M. C. Taylor, J. F. Whitte, G. P. Vincent and G. I. Cunnigham, *Ind. Eng. Chem.*, 1940, **32**, 899–903.

45 N. F. Gray, in *Microbiology of Waterborne Diseases*, ed. S. L. Percival, M. V. Yates, D. W. Williams, R. M. Chalmers and N. F. Gray, Academic Press, London, 2nd edn, 2014, pp. 591–598.

46 E. M. Aieta and P. V. Roberts, *Environ. Sci. Technol.*, 1986, **20**, 50–55.

47 A. K. Horva, *Inorg. Chem.*, 2008, **47**, 7914–7920.

48 A. Earnshaw and N. N. Greenwood, *Chemistry of the Elements*, Elsiver, Burlington, MA, 2nd edn, 1997, vol. 60.

49 C. Tarimci, R. D. Rosenstein and E. Schempp, *Acta Crystallogr., Sect. B: Struct. Crystallogr. Cryst. Chem.*, 1976, **32**, 610–612.

50 V. Tazzoli, V. Riganti, G. Giuseppetti and A. Coda, *Acta Crystallogr., Sect. B: Struct. Crystallogr. Cryst. Chem.*, 1975, **31**, 1032–1037.

51 N. Langerman, *ACS Chem. Health Saf.*, 2021, **28**, 402–409.

52 *CRC handbook of chemistry and physics*, CRC Press, Boca Raton, 2004, vol. 85.

53 M. A. Busch, *Reference Module in Chemistry, Molecular Sciences and Chemical Engineering*, Elsevier, 2018.

54 F. A. Cotton, G. Wilkinson, C. A. Murillo and M. Bochmann, *Advanced inorganic chemistry*, John Wiley & Sons, Chichester, 5th edn, 1988.

55 E. M. Aieta and P. V. Roberts, *Environ. Sci. Technol.*, 1986, **20**, 50–55.

56 R. G. Kieffer and G. Gordon, *Inorg. Chem.*, 1968, **7**, 235–239.

57 R. G. Kieffer and G. Gordon, *Inorg. Chem.*, 1968, **7**, 239–244.

58 C. C. Hong and W. H. Rapson, *Can. J. Chem.*, 1967, **1**, 2053–2060.

59 S. K. Cary, M. Livshits, J. N. Cross, M. G. Ferrier, V. Mocko, B. W. Stein, S. A. Kozimor, B. L. Scott and J. Rack, *Inorg. Chem.*, 2018, **57**, 3782–3797.

60 V. Bondet, W. Brand-Williams and C. Berset, *LWT – Food Sci. Technol.*, 1997, **30**, 609–615.

61 G. V. Buxton, C. L. Greenstock, W. P. Helman and A. B. Ross, *J. Phys. Chem. Ref. Data*, 1988, **17**, 513–886.

62 C. Liang and C. J. Bruell, *Ind. Eng. Chem. Res.*, 2008, **47**, 2912–2918.

63 S. Ašperger, *Chemical Kinetics and Inorganic Reaction Mechanisms*, Plenum Publishers, New York, 2nd edn, 2003.

64 X. Yang, Z. Zheng, J. Hu, J. Qu, D. Ma, J. Li, C. Guo and C. M. Li, *iScience*, 2021, **24**, 103500.

65 H. A. Young and W. C. Bray, *J. Am. Chem. Soc.*, 1932, **54**, 4284–4296.

66 G. B. Kolski and D. W. Margerum, *Inorg. Chem.*, 1969, **8**, 1125–1131.

67 W. C. Bray and H. A. Liebhafsky, *J. Am. Chem. Soc.*, 1935, **57**, 51–56.

68 S. K. Patil, V. V. Ramakrishna and M. V. Ramaniah, *Coord. Chem. Rev.*, 1978, **25**, 133–171.

69 D. Cohen and B. Taylor, *J. Inorg. Nucl. Chem.*, 1961, **22**, 151–153.

70 P. R. Danesi, R. Chiarizia, G. Scibona and G. D'Alessandro, *J. Inorg. Nucl. Chem.*, 1971, **33**, 3503–3510.

71 M. R. Wright, *An Introduction to Chemical Kinetics*, John Wiley & Sons, Ltd, Hoboken, 2004, vol. 8.

72 G. B. Skinner, in *Introduction to Chemical Kinetics*, ed. G. B. Skinner, Academic Press, Dayton, 1974, pp. 108–140.

73 D. F. Swinehart, *J. Chem. Educ.*, 1962, **39**, 333.